

Stable and metastable Si negative-U centers in AlGaN and AlN

Xuan Thang Trinh, Daniel Nilsson, Ivan Gueorguiev Ivanov, Erik Janzén, Anelia Kakanakova-Georgieva and Nguyen Tien Son

Linköping University Post Print



N.B.: When citing this work, cite the original article.

Original Publication:

Xuan Thang Trinh, Daniel Nilsson, Ivan Gueorguiev Ivanov, Erik Janzén, Anelia Kakanakova-Georgieva and Nguyen Tien Son, Stable and metastable Si negative-U centers in AlGaN and AlN, 2014, Applied Physics Letters, (105), 16, 162106-1-162106-4.

<http://dx.doi.org/10.1063/1.4900409>

Copyright: American Institute of Physics (AIP)

<http://www.aip.org/>

Postprint available at: Linköping University Electronic Press

<http://urn.kb.se/resolve?urn=urn:nbn:se:liu:diva-112407>

Stable and metastable Si negative-U centers in AlGaN and AlN

Xuan Thang Trinh, Daniel Nilsson, Ivan G. Ivanov, Erik Janzén, Anelia Kakanakova-Georgieva, and Nguyen Tien Son

Citation: [Applied Physics Letters](#) **105**, 162106 (2014); doi: 10.1063/1.4900409

View online: <http://dx.doi.org/10.1063/1.4900409>

View Table of Contents: <http://scitation.aip.org/content/aip/journal/apl/105/16?ver=pdfcov>

Published by the [AIP Publishing](#)

Articles you may be interested in

[Negative-U behavior of the Si donor in Al_{0.77}Ga_{0.23}N](#)

Appl. Phys. Lett. **103**, 042101 (2013); 10.1063/1.4816266

[The complex impact of silicon and oxygen on the n-type conductivity of high-Al-content AlGaN](#)

Appl. Phys. Lett. **102**, 132113 (2013); 10.1063/1.4800978

[Deep centers and persistent photocapacitance in AlGaN/GaN high electron mobility transistor structures grown on Si substrates](#)

J. Vac. Sci. Technol. B **31**, 011211 (2013); 10.1116/1.4773057

[Spatial distribution of deep level defects in crack-free AlGaN grown on GaN with a high-temperature AlN interlayer](#)

J. Appl. Phys. **100**, 123101 (2006); 10.1063/1.2402964

[Photoluminescence studies of impurity transitions in AlGaN alloys](#)

Appl. Phys. Lett. **89**, 092107 (2006); 10.1063/1.2337856

The advertisement features a 3D simulation of a mechanical part with a red-to-blue color gradient. The text 'Over 600 Multiphysics Simulation Projects' is prominently displayed in white and blue. A blue button with the text 'VIEW NOW >>' is located in the bottom right corner. The COMSOL logo is also present in the bottom right corner.

Over **600** Multiphysics Simulation Projects

[VIEW NOW >>](#)

COMSOL

Stable and metastable Si negative-U centers in AlGa_xN and AlN

Xuan Thang Trinh, Daniel Nilsson, Ivan G. Ivanov, Erik Janzén,
 Anelia Kakanakova-Georgieva, and Nguyen Tien Son

Department of Physics, Chemistry and Biology, Linköping University, SE-58183 Linköping, Sweden

(Received 5 August 2014; accepted 8 October 2014; published online 23 October 2014)

Electron paramagnetic resonance studies of Si-doped Al_xGa_{1-x}N (0.79 ≤ x ≤ 1.0) reveal two Si negative-U (or DX) centers, which can be separately observed for x ≥ 0.84. We found that for the stable DX center, the energy |E_{DX}| of the negatively charged state DX⁻, which is also considered as the donor activation energy, abruptly increases with Al content for x ~ 0.83–1.0 approaching ~240 meV in AlN, whereas E_{DX} remains to be close to the neutral charge state E_d for the metastable DX center (~11 meV below E_d in AlN). © 2014 AIP Publishing LLC.

[<http://dx.doi.org/10.1063/1.4900409>]

High-efficiency compact deep-ultraviolet (UV) light sources such as light-emitting diodes and laser diodes for replacing low-efficiency and toxic gas lasers and mercury lamps used in water/air purification and disinfection or high-resolution photolithography have so far been developed based on AlN¹ and high-Al-content AlGa_xN.^{2,3} In such devices, high *n*-type conductivity is required. Silicon (Si) is used for the *n*-type doping but achieving highly conductive *n*-type Al_xGa_{1-x}N for x ≥ 0.70 is proven difficult. A sharp increase in the donor activation energy E_a⁴⁻⁶ and resistivity⁷ was reported for Si-doped Al_xGa_{1-x}N with x in the range of ~0.8–1.0. Carrier compensation by deep level defects, including deep Si DX (or negative-U) centers, has often been speculated.

Different calculations^{8,9} suggested Si to be a deep DX center in AlN. In the neutral charge state d⁰, a Si donor prefers to capture another electron and undergoes a large lattice relaxation, relaxing to its lower-lying negatively charged state DX⁻ according to the process: 2d⁰ → DX⁻ + d⁺ (here d⁺ is the positive charge state of the donor). Depending on the energy separation between the d⁰ and DX⁻ state, E_d–E_{DX}, is small or large compared to E_d; such a DX donor may behave as a shallow donor or a self-compensation center. Some hybrid functional calculations in AlN^{10,11} have found two configurations of Si DX donors: a stable DX₁ center with the broken Si–N bond along the *c* axis and a metastable DX₂ center related to one of three equivalent broken Si–N basal bonds. A more recent calculation predicted no DX-like behavior for Si in AlN and suggested that the *n*-type conductivity in AlN is caused by the cluster of four Si and an Al vacancy, V_{Al}–4Si, which is predicted to have a formation energy lower than that of the substitutional Si_{Al} donor.¹²

In a Raman spectroscopy study of GaN:Si under hydrostatic pressure, where the results can be transferred to Al_xGa_{1-x}N, no DX behavior was detected for x up to ~0.56.¹³ A later transport study¹⁴ suggested Si to be a DX center in Al_xGa_{1-x}N for x ≥ 0.5. In electron paramagnetic resonance (EPR) studies of Si-doped Al_xGa_{1-x}N (x ≥ 0.75)¹⁵ and AlN,¹⁶ the requirement of illumination at low temperatures (T < 60 K) for detecting the signal of the shallow donor was explained by the DX-like nature of Si. However, a later EPR study suggested that Si is a shallow donor in AlN and explained the failure of detecting its EPR signal in darkness

to be due to carrier compensation by deeper electron traps.¹⁷ The DX behavior was also reported for donors in undoped AlN¹⁸ which was later suggested to be related to the oxygen donor O_N.¹⁹ A recent EPR study of Si-doped Al_{0.77}Ga_{0.23}N²⁰ suggested that Si forms a stable DX⁻ state already for x ~ 0.77 but its influence on the *n*-type conductivity is not essential since the neutral state E_d lies only ~3 meV above the Fermi level E_F. In AlN, the energy separation E_d–E_F increases to ~78 meV.²¹ A recent hybrid functional calculation²² suggested that Si transforms to a DX center in AlGa_xN when the Al content reaches ~94%.

In this letter, EPR was used to study Si-doped Al_xGa_{1-x}N epitaxial layers, 0.79 ≤ x ≤ 1.0, grown by metal-organic chemical vapor deposition (MOCVD). The energy levels of DX⁻ and d⁰ states were determined from the temperature dependence of the Si concentration in the neutral state d⁰. From EPR experiments, we found the existence of two DX configurations of the Si donor for x ≥ 0.84: one with E_{DX} remaining close to E_d and the other with E_{DX} increasing linearly and drastically with the Al content. The drastic deepening of the stable DX center explains the sharp decrease of the conductivity often observed in transport measurements.

Si-doped Al_xGa_{1-x}N (0.79 ≤ x ≤ 1) layers with typical thickness of ~400–600 nm were grown by MOCVD on semi-insulating 4H-SiC substrates using silane (SiH₄) as dopant gas. Further details about the growth processes can be found elsewhere.^{23,24} The Al content, the thickness of the Al_xGa_{1-x}N:Si layers, and the atomic concentration of Si, O, and C were determined by secondary ion mass spectrometry (SIMS) by Evans Analytical Group (the notation [] is used in this paper to denote the concentration obtained from SIMS). In all studied samples, the concentration of Si was kept at [Si] ~ 2 × 10¹⁸ cm⁻³ while the concentrations of O and C were reduced to the detection limit of SIMS ([O] ~ [C] ~ 2 × 10¹⁷ cm⁻³) so that the influence of these impurities on the free-carrier concentration and EPR results can be neglected. At such a moderate Si doping level, layers usually have good morphology and conductivity, which are important factors to guarantee the observation of good EPR signal of the shallow donor in darkness (It is known from our previous study²³ that in layers with high Si doping and pit-populated morphology, neither conductivity nor EPR signal can be detected). For the studied samples, XRD

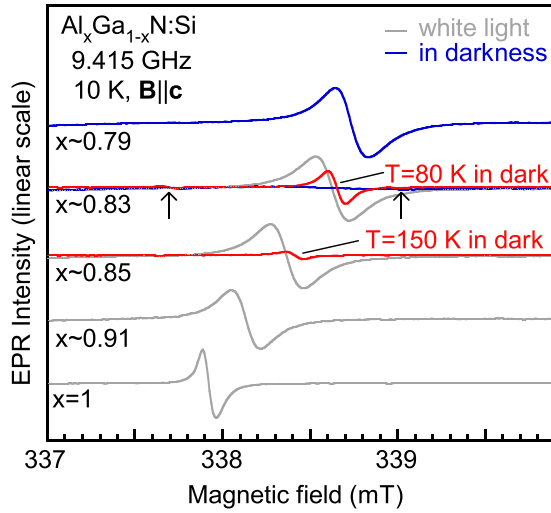


FIG. 1. EPR spectra of $\text{Al}_x\text{Ga}_{1-x}\text{N}:\text{Si}$ measured at 10 K for $\mathbf{B}\parallel\mathbf{c}$. The EPR spectra of $\text{Al}_{0.83}\text{Ga}_{0.17}\text{N}:\text{Si}$ measured at 80 K and $\text{Al}_{0.85}\text{Ga}_{0.15}\text{N}:\text{Si}$ at 150 K in darkness were also given for comparison. The EPR signal of the Si shallow donor could be detected in darkness in $\text{Al}_x\text{Ga}_{1-x}\text{N}:\text{Si}$ layers with $x \sim 0.79$, while in layers with $x \geq 0.83$, the observation of the EPR signal required illumination or thermal excitation at elevated temperatures. The arrows indicate the positions of the Si hyperfine lines of the carbon vacancy defect²⁶ from the 4H-SiC substrate.

rocking curves of the (0002) and (10 $\bar{1}$ 2) plane reflections were measured with full width at half maximum of about 100–200 arcsec and 380–480 arcsec, respectively. Using the method given by Lee *et al.*²⁵ the screw and edge dislocation densities were estimated to be about $(4 \pm 2) \times 10^7 \text{ cm}^{-3}$ and $(2 \pm 1) \times 10^9 \text{ cm}^{-3}$, respectively. EPR measurements were performed on an X-band (~ 9.4 GHz) E500 Bruker spectrometer equipped with a continuous He-flow cryostat, allowing the regulation of the sample temperature from 4 to 295 K. For illumination, 200 W-halogen or 150 W-xenon lamps was used as a light source. The donor concentration or the number of spins was determined using the spin counting application provided and calibrated by Bruker.

In $\text{Al}_{0.79}\text{Ga}_{0.21}\text{N}:\text{Si}$ layers, the signal of the shallow donor could be detected in darkness at 10 K (Fig. 1) similar to the case of $\text{Al}_{0.77}\text{Ga}_{0.23}\text{N}:\text{Si}$ for which the neutral state d^0 is ~ 3 meV above the Fermi level,²⁰ and the thermal-induced population on d^0 at low temperatures is detectable by EPR. In layers with $x \sim 0.83$ –0.85, the EPR signal can still be detected in darkness, but only at elevated temperatures

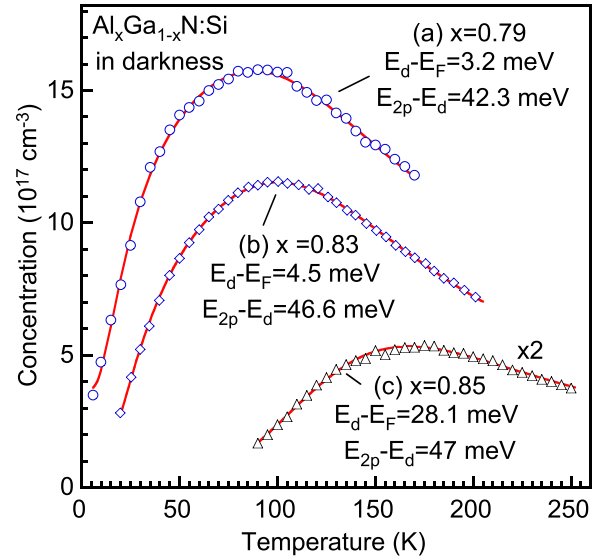


FIG. 2. Temperature dependence of the donor concentration in the d^0 state in darkness in $\text{Al}_x\text{Ga}_{1-x}\text{N}:\text{Si}$ layers with (a) $x \sim 0.79$, (b) $x \sim 0.83$ and (c) $x \sim 0.85$. The donor concentration in the $\text{Al}_{0.85}\text{Ga}_{0.15}\text{N}:\text{Si}$ layer was shown in $\times 2$ scale. The solid curves represent the fits using Eq. (2).

($T \geq 30$ K for $x \sim 0.83$ and $T \geq 80$ K for $x \sim 0.85$). Since the Si-doped layer in all samples is thin (~ 400 –600 nm), the total number of Si in the neutral state induced by thermal energy with the Al content exceeding ~ 0.85 is below the detection limit of EPR. In these layers, the EPR signal of the Si donor could only be detected under or after illumination with light of photon energies in the range ~ 1.6 –2.9 eV depending on the Al content.

Figure 2 shows the temperature dependence of the concentration of the shallow donor $n(T)$ in the neutral charge state d^0 in $\text{Al}_x\text{Ga}_{1-x}\text{N}:\text{Si}$ layers of $x \sim 0.79$ –0.85 determined from EPR measurements in darkness. The measurements performed with the microwave power varying in the range from 0.1 mW to 4 mW gave the same $n(T)$ values, indicating that under these measurement conditions, no partial saturation occurred and the EPR signal was proportional to $n(T)$. In all samples, $n(T)$ is smallest at the lowest temperature and increases to a maximum at a certain temperature. Such temperature dependence is typical for a DX center. The average population on the d^0 state in a negative-U center can be described by the Boltzmann distribution²⁷ with including the excited states^{28,29}

$$n(T) \propto \frac{N2e^{-(E_d-E_F)/k_B T}}{1 + 2e^{-(E_d-E_F)/k_B T} + e^{-\{2E_d-(E_d-E_{DX})-2E_F\}/k_B T} + \sum_i G_i e^{-(E_i-E_F)/k_B T}} \quad (1)$$

Here, N is the total donor concentration, k_B is the Boltzmann constant, E_i and G_i are the energy level of excited states and their degenerate factors, respectively. It has been shown that in a negative-U center, the Fermi level is pinned at the middle of E_d and E_{DX} levels (i.e., $E_F - E_{DX} = E_d - E_F$) almost

independently of the electron density on the levels.^{27,29} A recent calculation of Si DX center in AlGa N and AlN²² also showed that the Fermi level is located at the middle between E_d and E_{DX} levels. Thus, with considering only the first excited state 2p, Eq. (1) can be rewritten as

$$n(T) \propto \frac{N}{1 + 0.5e^{(E_d - E_F)/k_B T} + 0.5e^{(E_F - E_{DX})/k_B T} + Ce^{-(E_{2p} - E_d)/k_B T}}, \quad (2)$$

$$n(T) \propto \frac{N}{1 + e^{(E_d - E_F)/k_B T} + Ce^{-(E_{2p} - E_d)/k_B T}}.$$

Here, $E_{2p} - E_d$ is the energy distance from d^0 (E_d or E_{1s}) to first excited state $2p$, and C is a factor taking into account the thermal excitation from the first excited state to higher-lying excited states (including their degeneration factors). From the best fits to experimental data using Eq. (2), $E_d - E_F$ was found to increase drastically from ~ 3 – 5 meV for $x = 0.79$ – 0.83 to ~ 28 meV for $x \sim 0.85$. The value $E_{2p} - E_d$ was determined to be ~ 42.3 meV for $x \sim 0.79$ and ~ 47 meV for $x = 0.85$. Assuming that the neutral state E_d and excited states of the Si donor follow the effective mass theory (EMT), i.e., the E_d/i^2 rule ($i = 1, 2, \dots, n$) or $E_{2p} \sim E_d/4$ and $|E_{2p} - E_d| = |(E_d/4) - E_d| = 3|E_d|/4$, we can estimate $|E_d|$ as: $|E_d| = 4|E_{2p} - E_d|/3 \sim 56.8, \sim 62, 63.3$ and ~ 64.6 meV for $x \sim 0.79, \sim 0.83, 0.84$, and ~ 0.85 , respectively. In all studied samples, the values of the total concentration of the Si donor obtained from the fits are in the range of 3 – $4 \times 10^{18} \text{ cm}^{-3}$, which are higher than the Si concentration obtained from SIMS ($\sim 2 \times 10^{18} \text{ cm}^{-3}$). This systematic overestimation of the donor concentration by EPR may be due to the calibration in Bruker program. The degeneration factor C is about 20 – 30 for the Al content x in the range of 0.79 – 0.83 and $C \sim 110$ for $x = 0.85$. In higher Al-content samples, the decrease of $n(T)$ occurs at higher temperatures at which electrons can be more efficiently moved to excited states. Therefore, higher values of the C factor are expected for higher Al-content samples.

Using the effective mass values and dielectric constants interpolated from GaN and AlN as described in previous studies²⁰ to calculate the donor ionization energy in $\text{Al}_x\text{Ga}_{1-x}\text{N}$, we obtained the EMT values for different Al

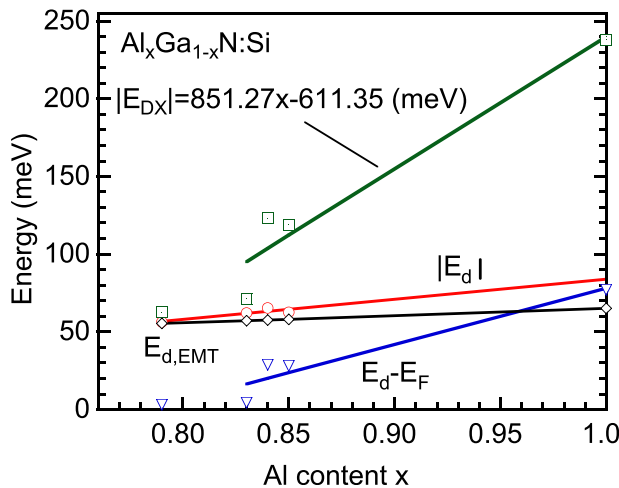


FIG. 3. The linear dependence on the Al content of the ionization energy of the neutral charge state d^0 (E_d), the DX^- state ($|E_{DX}| = E_d$), and the energy separation $E_d - E_F$ in $\text{Al}_x\text{Ga}_{1-x}\text{N}:\text{Si}$ with $0.79 \leq x \leq 1$. The dependence of the ionization energy $E_{d,EMT}$ on the Al content obtained from EMT calculations is also plotted for comparison. The $|E_{DX}|$ value for AlN was measured in an unintentionally Si-doped AlN bulk sample similar to the one previously used in Ref. 21.

contents $E_{d,EMT}$. The calculated $E_{d,EMT}$ values and the $|E_d|$ values obtained from experiments are shown in Fig. 3. Extrapolation from the linear fit to the obtained $|E_d|$ values gives $|E_d| \sim 84$ meV for AlN with a deviation of ~ 19 meV from the corresponding EMT value (65.2 meV).

The energy separation $E_d - E_F$ was determined to be: $\sim 3.2, \sim 4.5, \sim 28.8$ and 28.1 meV for $\text{Al}_x\text{Ga}_{1-x}\text{N}$ layers with $x \sim 0.79, \sim 0.83, \sim 0.84$ and ~ 0.85 , respectively. In our previous studies,^{20,21} the term related to the DX^- state in the partition function, i.e., the third term in the denominator of Eq. (1), was neglected. Using Eq. (2), we analyzed the data in Refs. 20 and 21 and obtained small changes, e.g., $E_d - E_F \sim 2.3$ and ~ 77 meV compared to the values of ~ 2.8 and ~ 78 meV for Si in $\text{Al}_{0.77}\text{Ga}_{0.23}\text{N}$ and AlN, respectively.^{20,21} The E_{DX} levels of Si in $\text{Al}_x\text{Ga}_{1-x}\text{N}$ with $x \sim 0.79, \sim 0.83, \sim 0.84, \sim 0.85$ and in AlN were estimated to be $|E_{DX}| \sim |E_d| + 2|E_d - E_F| \sim 63, \sim 71, \sim 123, \sim 119$ and ~ 238 meV, respectively. The obtained $|E_d - E_F|$ and $|E_{DX}|$ values are shown in Fig. 3. The best fit to $|E_{DX}(x)|$ values for $x \geq 0.83$ gave the dependence of $|E_{DX}(x)|$ on the Al content as

$$|E_{DX}(x)| = 851.27x - 611.35 \text{ (meV)}. \quad (3)$$

For $x \geq 0.83$, the observation of strong EPR signals of the Si donor at low temperatures required illumination. After illumination, the EPR signals of the Si donor were persistent for hours in darkness for $T \leq 50$ K. We found that $n(T)$ measured

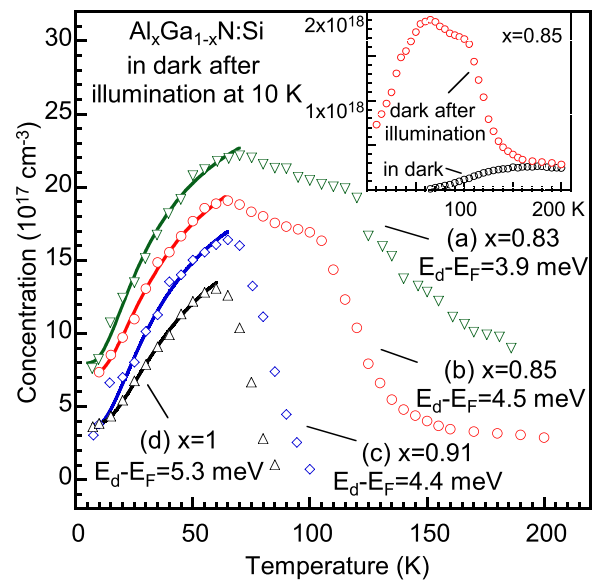


FIG. 4. Temperature dependence of the donor concentration in the d^0 state in darkness after illumination at 10 K in Si-doped $\text{Al}_x\text{Ga}_{1-x}\text{N}$ with (a) $x \sim 0.83$, (b) $x \sim 0.85$, (c) $x \sim 0.91$ and (d) in Si-doped AlN. The solid curves represent the fits. The inset shows the temperature dependences of the donor concentration in darkness and in darkness after illumination at 10 K in $\text{Al}_{0.85}\text{Ga}_{0.15}\text{N}:\text{Si}$ in the same scale for comparison.

in darkness after illumination increased with increasing temperature and reached its maximum at $T \sim 60\text{--}70\text{ K}$, which was close to the SIMS value [Si] for all samples, and then rapidly decreased, approaching the values measured in darkness without prior illumination (see the inset of Fig. 4).

The increase of $n(T)$ in darkness after illumination is typical for a DX center. Thus, the EPR signal measured at low temperatures ($T < 60\text{ K}$) after illumination should be from another DX configuration whose DX^- level lies higher than that of the center detected in darkness at higher temperatures. At $T < 60\text{ K}$, electrons are confined in this higher-lying (or metastable) DX configuration. When temperature exceeds 60 K , thermal energy is enough to help electrons to overcome the barrier between the two DX configurations and to relax to the lower-lying (or stable) DX configuration, leading to the sharp drop of $n(T)$ (Fig. 4). We label the stable and metastable DX configurations as DX1 and DX2, respectively. For DX2, the temperature dependence of $n(T)$ in the temperature range below 60 K can be described by Eq. (2) but without the third term in the denominator since the thermal energy is not enough to excite electrons to the excited states. In this case, electrons are confined within the metastable DX2 configuration, and the Fermi level E_F is local. For all samples with $x \geq 0.84$, the energy separation $E_d - E_F$ obtained from the best fit is in the range of $\sim 3.9\text{--}5.3\text{ meV}$ (Fig. 4). These values are much smaller than the corresponding values determined in darkness ($\sim 28\text{ meV}$ or larger), indicating that in this metastable DX2 configuration, the DX^- state is much closer to the d^0 state ($E_d - E_{\text{DX}} \sim 8\text{--}11\text{ meV}$ for $x \sim 0.83\text{--}1.0$, respectively). Our observation of two distinguishable DX configurations of the Si donor in $\text{Al}_x\text{Ga}_{1-x}\text{N}$ for $x \geq 0.84$ supports the theoretical prediction by Silvestri *et al.* for Si in AlN.^{10,11}

In darkness, transport measurements would probe the stable DX1 center. For AlN, our value $|E_{\text{DX}}| \sim 240\text{ meV}$ is close to the activation energy determined from transport measurements for Si: $E_a \sim 238\text{--}254\text{ meV}$ ³⁰ and $E_a \sim 250\text{ meV}$.^{5,6} The Fermi level found in our experiments for AlN of $\sim 160\text{ meV}$ below the conduction band minimum is also close to the $(+|-)$ level of Si ($\sim E_C - 150\text{ meV}$), where the Fermi level is pinned, determined recently from calculations by Gordon *et al.*²² From Eq. (3), the $|E_{\text{DX}}|$ value for Si in $\text{Al}_x\text{Ga}_{1-x}\text{N}$ with x in the range of $\sim 0.83\text{--}1.0$ can be interpolated, for example $|E_{\text{DX}}| \sim 189\text{ meV}$ for $x \sim 0.94$ which is close to the corresponding E_a value of $\sim 200\text{ meV}$ determined by Borisov *et al.*⁵

In summary, our EPR characterization of Si-doped $\text{Al}_x\text{Ga}_{1-x}\text{N}$, $0.79 \leq x \leq 1.0$, showed that up to $x \sim 0.83$, the DX^- state is still close to the neutral state E_d ($E_d - E_{\text{DX}} \sim 9\text{ meV}$) and Si behaves rather similar to a shallow effective-mass donor. For $x \geq 0.84$, two DX centers could be separately observed. For the stable DX1 center, the activation energy $E_a \sim |E_{\text{DX}}|$ increases drastically and linearly from $\sim 71\text{ meV}$ in $\text{Al}_{0.83}\text{Ga}_{0.17}\text{N}$ to $\sim 240\text{ meV}$ in AlN. For the metastable DX2 center, the E_{DX} level remains to be close to the neutral charge state d^0 ($\sim 11\text{ meV}$ below E_d in AlN). The dependence of the E_{DX} level of the stable DX1 center on the Al content explains well the sudden increase of the

resistivity in high-Al-content AlGa_N reported by transport measurements.

Support from the Swedish Energy Agency, Swedish Research Council (VR), Linköping Linnaeus Initiative for Novel Functional Materials (VR), the Swedish Government Strategic Research Area Grant in Materials Science (Advanced Functional Materials), and Knut and Alice Wallenberg Foundation is gratefully acknowledged. A.K.G. acknowledges support from the Swedish Governmental Agency for Innovation Systems (VINNOVA).

- ¹Y. Taniyasu, M. Kasu, and T. Makimoto, *Nature* **441**, 325 (2006).
- ²Z. Lochner, T.-T. Kao, Y.-S. Liu, X.-H. Li, M. M. Satter, S.-C. Shen, P. D. Yoder, J.-H. Ryou, R. D. Dupuis, Y. Wei, H. Xie, A. Fischer, and F. A. Ponce, *Appl. Phys. Lett.* **102**, 101110 (2013).
- ³N. Norimichi, H. Hirayama, T. Yatabe, and N. Kamata, *Phys. Status Solidi C* **6**, S459 (2009).
- ⁴M. L. Nakarmi, K. H. Kim, K. Zhu, J. Y. Lin, and H. X. Jiang, *Appl. Phys. Lett.* **85**, 3769 (2004).
- ⁵B. Borisov, V. Kuryatkov, Y. Kudryavtsev, R. Asomoza, S. Nikishin, D. Y. Song, M. Holtz, and H. Temkin, *Appl. Phys. Lett.* **87**, 132106 (2005).
- ⁶R. Collazo, S. Mita, J. Xie, A. Rice, J. Tweedie, R. Dalmau, and Z. Sitar, *Phys. Status Solidi C* **8**, 2031 (2011).
- ⁷F. Mehnke, T. Wernicke, H. Pingel, C. Kuhn, C. Reich, V. Kueller, A. Knauer, M. Lapeyrade, M. Weyers, and M. Kneissl, *Appl. Phys. Lett.* **103**, 212109 (2013).
- ⁸C. H. Park and D. J. Chadi, *Phys. Rev. B* **55**, 12995 (1997).
- ⁹P. Boguslawski and J. Bernholc, *Phys. Rev. B* **56**, 9496 (1997).
- ¹⁰L. Silvestri, K. Dunn, S. Prawer, and F. Ladouceur, *Appl. Phys. Lett.* **99**, 122109 (2011).
- ¹¹L. Silvestri, K. Dunn, S. Prawer, and F. Ladouceur, *Europhys. Lett.* **98**, 36003 (2012).
- ¹²D. F. Hevia, C. Stampfl, F. Viñes, and F. Illas, *Phys. Rev. B* **88**, 085202 (2013).
- ¹³C. Wetzel, T. Suski, J. W. Ager III, E. R. Weber, E. E. Haller, S. Fischer, B. K. Meyer, R. J. Molnar, and P. Perlin, *Phys. Rev. Lett.* **78**, 3923 (1997).
- ¹⁴C. Skierbiszewski, T. Suski, M. Leszczynski, M. Shin, M. Skowronski, M. D. Bremser, and R. F. Davis, *Appl. Phys. Lett.* **74**, 3833 (1999).
- ¹⁵M. W. Bayerl, M. S. Brandt, T. Graf, O. Ambacher, J. A. Majewski, M. Stutzmann, D. J. As, and K. Lischka, *Phys. Rev. B* **63**, 165204 (2001).
- ¹⁶R. Zeisel, M. W. Bayerl, S. T. B. Goennenwein, R. Dimitrov, O. Ambacher, M. S. Brandt, and M. Stutzmann, *Phys. Rev. B* **61**, R16283 (2000).
- ¹⁷K. Irmscher, T. Schulz, M. Albrecht, C. Hartmann, J. Wollweber, and R. Fornari, *Physica B* **401–402**, 323 (2007).
- ¹⁸S. B. Orlinskii, J. Schmidt, P. G. Baranov, M. Bickermann, B. Epelbaum, and A. Winnacker, *Phys. Rev. Lett.* **100**, 256404 (2008).
- ¹⁹V. A. Soltamov, I. V. Ilyin, A. A. Soltamova, E. N. Mokhov, and P. G. Baranov, *J. Appl. Phys.* **107**, 113515 (2010).
- ²⁰X. T. Trinh, D. Nilsson, I. G. Ivanov, E. Janzén, A. Kakanakova-Georgieva, and N. T. Son, *Appl. Phys. Lett.* **103**, 042101 (2013).
- ²¹N. T. Son, M. Bickermann, and E. Janzén, *Appl. Phys. Lett.* **98**, 092104 (2011); *Phys. Status Solidi C* **8**, 2167 (2011).
- ²²L. Gordon, J. L. Lyons, A. Janotti, and C. G. Van De Walle, *Phys. Rev. B* **89**, 085204 (2014).
- ²³A. Kakanakova-Georgieva, D. Nilsson, X. T. Trinh, U. Forsberg, N. T. Son, and E. Janzén, *Appl. Phys. Lett.* **102**, 132113 (2013).
- ²⁴A. Kakanakova-Georgieva, D. Nilsson, and E. Janzén, *J. Cryst. Growth* **338**, 52 (2012).
- ²⁵S. R. Lee, A. M. West, A. A. Allerman, K. E. Waldrip, D. M. Follstaedt, P. P. Provencio, D. D. Koleske, and C. R. Abernathy, *Appl. Phys. Lett.* **86**, 241904 (2005).
- ²⁶T. Umeda, J. Isoya, N. Morishita, T. Ohshima, T. Kamiya, A. Gali, P. Deák, N. T. Son, and E. Janzén, *Phys. Rev. B* **70**, 235212 (2004).
- ²⁷D. Adler and E. J. Yoffa, *Phys. Rev. Lett.* **36**, 1197 (1976).
- ²⁸N. W. Ashcroft and N. D. Mermin, *Solid State Physics* (Thomson Learning, London, 1976), p. 581.
- ²⁹D. C. Look, *Phys. Rev. B* **24**, 5852 (1981).
- ³⁰Y. Taniyasu, M. Kasu, and T. Makimoto, *Appl. Phys. Lett.* **85**, 4672 (2004).